

1 **Test**

2 **Alexander Beck¹, Jan Henneberger¹, and Ulrike Lohmann¹**

3 ¹Institute for Atmospheric and Climate Sciences, ETH Zurich, Zurich, Switzerland

4 **Key Points:**

- 5 • In-situ measurements of microphysical cloud properties with a holographic Imager
6 • Influence of in-situ cloud observations at mountain top stations by ground based ice
7 enhancement processes
8 •

9 **Abstract**

10 In-situ cloud observations at mountain-top research station regularly measure ice crystal
 11 number concentrations (ICNCs) orders of magnitudes higher than expected from mea-
 12 surements or simulations of ice nuclei particle concentrations. Several studies suggest
 13 mountain-top in-situ measurements are influenced by surface-based ice-enhancement pro-
 14 cess, e.g. blowing snow, hoar frost or riming on snow covered trees, rocks and the remain-
 15 ing snow surface. A strong influence of in-situ observations on mountain-top stations by
 16 surface-based ice-enhancement processes may limit relevance of such measurements and
 17 could have an impact on orographic clouds.

18 This study assesses the influence of surface-based ice-enhancement processes on
 19 in-situ cloud observations at the Sonnblick Observatory in the Hohen Tauern Region,
 20 Austria. Vertical profiles of ICNCc above a snow covered surface were observed up to
 21 a height of 10 m. A decrease of the ICNC by at least a factor of two is observed, if the
 22 maximum ICNC is larger than 100I^{-1} . This decrease extended up to one order of mag-
 23 nitude during in cloud conditions and reached its maximum of more than two orders of
 24 magnitudes when the station was not in cloud. ... These observations strongly suggest that
 25 mountain-top in-situ measurements poorly represent the true properties of the cloud in
 26 contact with the surface. They are influenced not only by surface-based ice-enhancement
 27 processes, but possibly also by ICNC enhancement due to turbulent layers above the sur-
 28 face.

29 **1 Introduction**

30 The microphysical properties (e.g. phase composition, cloud particle number con-
 31 centrations) and cloud processes are key parameters for the clouds lifetime, the cloud ex-
 32 tent, as well as the intensity of precipitation they produce [Rotunno and Houze, 2007]. For
 33 example, the phase composition influence the radiative properties of midlevel clouds in
 34 the temperature range between 0 to -35 °C. A pure ice cloud in this temperature regime
 35 reflects 17W m^{-2} more radiation than an pure liquid cloud [Lohmann, 2002]. A well rep-
 36 resentation of orographic mixed-phase clouds is therefore crucial for accurate weather pre-
 37 dictions in alpine terrain and improved climate models.

38 In-situ measurements are important to improve our understanding of microphysical
 39 properties and fundamental processes of orographic mixed-phase clouds [Baumgardner
 40 et al., 2011] and are frequently conducted at mountain-top research stations. Despite an
 41 improved understanding on the origin of ice crystals from nucleation (citation!!!!) as well
 42 as from secondary ice-multiplication processes [Field et al., 2017], the source of most of
 43 the ice crystals observed at mountain-top stations and their impact on the development of
 44 the cloud remains an enigma (citation!!!!).

45 In-situ observations with aircraft usually observe ICNC on the order of $1\text{-}10\text{I}^{-1}$
 46 [Gultepe et al., 2001], whereas at mountain-top research stations (e.g. Elk Mountain, USA
 47 or Jungfraujoch, Switzerland) or near the snow surface in the Arctic ICNCs of several
 48 hundreds to thousands per liter are frequently reported [Rogers and Vali, 1987; Lachlan-
 49 Cope et al., 2001; Lloyd et al., 2015]. Secondary ice multiplication processes like frag-
 50 mentation [Rangno and Hobbs, 2001] or the Hallett-Mossop process [Hallet and Mossop,
 51 1974] are usually ruled out as the source for the observed ice crystals due to the lack of
 52 large ice crystals, respectively large cloud droplets or the wrong temperature range. In-
 53 stead surface-based ice-enhancement processes are proposed to produce such enormous
 54 ICNCs. Rogers and Vali [1987] suggested two possible processes as a source for the ob-
 55 served ICNC: riming on trees, rocks and the snow surface or the lifting of snow particles
 56 from the surface, i.e. blowing snow. In addition, Lloyd et al. [2015] suggested hoar frost
 57 as a wind independent, surface-based ice-enhancement process to cause ICNCs larger than
 58 100I^{-1} for which they didn't observe a wind dependency as expected for blowing snow.

59 Although different studies are strife about the mechanisms to explain the measured high
 60 ICNCs, they agree on an strong influence by surface-based processes.

61 While the influence of mountain-top measurements by surface-based processes is
 62 widely accepted, the impact of re-suspended ice crystals on the development of super-
 63 cooled orographic clouds, e.g. a more rapid glaciation and enhanced precipitation, has not
 64 been studied extensively [Geerts *et al.*, 2015]. If the proposed surface-based ice-enhancement
 65 processes have the potential to impact the development of a cloud depends primarily on
 66 the penetration depth of the reseuspended particle into a cloud, i.e. the maximum height
 67 above the surface to which the particles get lifted.

68 The height dependency of blowing snow has been studied in the context of snow
 69 redistribution ("snow drift") and reduced visibility due to the re-suspended ice crystals
 70 by observing ice crystals up to several meters above the snow surface [Schmidt, 1982;
 71 Nishimura and Nemoto, 2005]. It has been reported that blowing snow occurs above a
 72 wind speed threshold that varies between 4 m s^{-1} and 13 m s^{-1} [Bromwich, 1988; Li and
 73 Pomeroy, 1997; Mahesh *et al.*, 2003; Déry and Yau, 1999]. Besides the wind speed, the
 74 concentration of blowing snow depends on the snowpack properties () and on the atmo-
 75 pheric conditions (current temperature, humidity) [Vionnet *et al.*, 2013]. Nishimura and
 76 Nemoto [2005] observed the ICNC up to a height of 9.6 m and found that the ICNCs usu-
 77 ally decrease to as low as 1-10 particles per liter. During a precipitation event, the relative
 78 importance of the small ice crystals below $< 100 \mu\text{m}$ decreases from nearly 100 % at 1.1 m
 79 to below 20 % at 9.6 m. The rapid decrease of ICNCs with height observed by these
 80 studies may limit the impact of blowing snow on orographic clouds. However, most of these
 81 studies were conducted in dry air conditions where ice crystals undergo rapid sublimation
 82 [Yang and Yau, 2008], which may limit the applicability of these results.

83 *Lloyd et al.* [2015] suggested that vapor grown ice crystals on the crystalline sur-
 84 face of the snow cover, i.e. hoar frost, may be detached by mechanical fracturing due to
 85 turbulence independent of wind speed. To our knowledge only one modelling study ex-
 86 exists, which asses the impact of haor frost on the development of a cloud. *Farrington et al.*
 87 [2015] implemented a flux of surface hoar crystals in the WRF (Weather Research and
 88 Forecasting) model based on a frost flower aerosol flux to simulate ICNCs measured at the
 89 Jungfraujoch by *Lloyd et al.* [2015]. They concluded, that the surface-based ice-crystals
 90 have a limiting impact on orographic clouds because the ice crystals are not advected high
 91 into the atmosphere. However, more measurements of ice-crystal fluxes from the snow
 92 covered surface are necessary to simulate the impact of surface-based ice-crystal enhance-
 93 ment processes on the development of orographic clouds [*Farrington et al.*, 2015].

94 In contrast to these finding, several remote sensing (i.e. satellite, lidar and radar)
 95 studies measured ice crystals advected as high as 1 km above the surface, which suggest
 96 an impact of surface-originated ice-crystals on clouds. Satellite observations of blow-
 97 ing snow from MODIS and CALIOP over the Antarctica [Palm *et al.*, 2011] observed
 98 layer thickness up to 1 km with an average thickness of 120 m for all observed blowing
 99 snow events. Similar observations from lidar measurements exist from the South Pole
 100 with an observed layer thickness of ice crystals of usually less than 400 m, but some rare
 101 cases when a subvisual layer exceeded a height of 1 km [Mahesh *et al.*, 2003]. However, a
 102 possible suspension of clear-sky precipitation could not be ruled out as a source of the
 103 observed ice crystal layers. Observations of layers of ice crystals from radar measure-
 104 ments on an aircraft in the vicinity of the Medicine Bow Mountains [Vali *et al.*, 2012]
 105 observed ground-layer snow clouds which where most of the time not visually detectable
 106 but produced a radar signal. Resuspended ice crystals from the surface or riming of cloud
 107 droplets at the surface can be the origin of the ice crystals in such ground-layer snow
 108 clouds. *Geerts et al.* [2015] presented evidence for ice crystals becoming lofted up to
 109 250 m in the atmosphere by boundary layer separation behind terrain crests and by hy-
 110 draulic jumps. Also evidence that ice crystals from the surface may lead to the glaciation
 111 of supercooled orographic clouds and enhanced precipitation were found. However, *Geerts*

112 *et al.* [2015] also mention the limitation of radar and lidar measurement to separate the
 113 small ice crystals produced by surface processes from the larger falling snow particles
 114 and more abundant cloud droplets. They even concluded, that "to explore BIP (blowing
 115 snow ice particle) lofting into orographic clouds, ice particle imaging devices need to be
 116 installed on a tall tower, or on a very steep mountain like the Jungfraujoch".

117 In this study we assess the influence of surface-based ice-enhancement processes
 118 on in-situ cloud observations at mountain-top stations and the a potential impact on oro-
 119 graphic mixed-phase clouds. Therefore, vertical profiles of the ICNC up to a height of
 120 10 m above the surface are observed for the first time in cloud at the Sonnblick Observa-
 121 tory. Ice crystals are recorded with the holographic imager HOLIMO, capable of observ-
 122 ing ice crystals larger than 25 μm [Beck *et al.*, 2017].

123 2 Field Measurements at the Sonnblick Observatory

124 2.1 Site description

125 This field campaign was conducted at the Sonnblick Observatory (SBO) situated at
 126 the summit of Mt. Sonnblick at 3106 masl (12°57'E, 47°3'N) in the Hohen Tauern Na-
 127 tional Park in the Austrian Alps. The SBO is a meteorological observatory operated all
 128 year by the ZAMG (Central Institute for Meteorology and Geodynamics). On the East and
 129 South the SBO is surrounded by large glacier fields with a moderate slope, whereas on the
 130 Northeast a steep wall of approximately 800 m descends to the valley (Fig. 1, right). Part
 131 of the SBO is a 15 m high tower used for meteorological measurements by the ZAMG.
 132 The data presented in this paper was collected during a field campaign in February 2017.

133 2.2 Instrumentation

134 The microphysical properties of clouds, hydrometeors and resuspended particles
 135 from the surface were observed with the holographic Imager HOLIMO, which is part of
 136 the HoloGondel platform [Beck *et al.*, 2017]. The holographic Imager was mounted on an
 137 elevator that was attached to the meteorological tower of the SBO (Fig. 2) to obtain verti-
 138 cal profiles of the microphysical properties up to a height of 10 m above the surface where
 139 the platform was repeatedly positioned at five different heights as indicated in Figure 2.
 140 The holographic imager HOLIMO had a distance of approximately 1.5 m from the tower
 141 on the east-northeast side of the tower (Fig. 1, right). The holographic imager HOLIMO
 142 captures the information of cloud particles in a three-dimensional volume on a single im-
 143 age. In this study a sample volume of 16 cm^3 with a length of 6 cm along the optical axis
 144 was examined. The data is averaged over 50 holograms and a total volume of 800 cm . The
 145 open source software HoloSuite [Fugal, 2017] is used to reconstruct the in-focus images
 146 of the particles. Particles smaller than 25 μmm are classified as liquid droplets, whereas
 147 particles larger than 25 μmm are separated in liquid droplets and ice crystals based on
 148 the shape of their 2D image. Similar to a study by Schlenzeck and Fugal [2017] the ice
 149 crystals were further visually classified into three different groups: regular, irregular and
 150 aggregates. Because the visual classification of several thousands of ice crystals is time
 151 consuming this sub-classification of ice crystals was done only for the profiles on Febru-
 152 ary 17th.

153 Meteorological data are available from the measurements by the ZAMG and the
 154 HoloGondel platform. The ZAMG measures one minute averages of temperature, rela-
 155 tive humidity and horizontal wind speed and direction at the top of the meteorological
 156 tower. Snow cover depth is daily manually observed by the operators of the SBO. Based
 157 on these measurements the change of the snow cover is calculated. However, this calcula-
 158 tion includes all the changes in the snow cover depth, e.g. snow drift, sublimation, melting
 159 and fresh snow. Daily measurements of the total precipitation are available on the North
 160 and South side of the SBO. A ceilometer located in the valley on the North of the SBO

161 measured the cloud base and cloud depth. An additional 3D Sonic Anemometer, which is
 162 part of the HoloGondel platform [Beck *et al.*, 2017], was mounted at the top of the meteo-
 163 rological tower. However, data is only available occasionally, because most of the time the
 164 heating of the Anemometer was not sufficient enough to prevent the build up of rime on
 165 the measurement arms.

166 3 Results

167 The data presented were observed on 4 February and 17 February 2017. Figure 3
 168 and 4 show an overview on the meteorological conditions on both days. The main differ-
 169 ence is the wind direction, which was South-West on 4 February and North on 17 Febru-
 170 ary.

171 3.1 4 February 2017

172 On 4 February a low pressure system moved eastwards from the Atlantic Ocean over
 173 northern France to western Germany, where it slowly dissipated. Influenced by this low
 174 pressure system the wind at the SBO predominantly came from West-Southwest and wind
 175 speeds between 10 and 25 m s⁻¹. In the late afternoon around 1900 UTC, when the low
 176 pressure system dissipated over western Germany, the wind direction changed to North
 177 and wind speeds decreased to a minimum of 5 m s⁻¹. After 1900 UTC wind speed in-
 178 creased again to up to 15 m s⁻¹. Starting from 0800 UTC the SBO was in cloud except
 179 for a short time interval between 1910 and 2020 UTC. The temperature didn't change
 180 much during the day and stayed between -10 and -9 °C until 1900 UTC when the wind
 181 direction changed to North and the temperature decreased to -11 °C at 22 UTC.

182 Between 0830 and 2200 UTC, a total of 24 vertical profiles were obtained. Because
 183 no data is available from the 3D Sonic Anenometer, only one minute averages of tem-
 184 perature, wind speed and direction are available from the ZAMG measurements (Fig. 3).
 185 Most of the profiles were obtained when the station was in cloud expect for four profiles
 186 between 1910 and 2020 UTC as indicated in Figure 3. The ICNC as a function of height
 187 summarized over 24 vertical profiles obtained on 4 February is shown in Figure 5. The
 188 ICNC reaches a maximum at 2.5 m above the surface. Compared to this maximum, the
 189 mean ICNC at a height of 10 m decreases by a factor of two and the median ICNC even by
 190 a factor of four. These observations suggest an influence of the measurements close to the
 191 snow surface by surface based ice crystal enhancement processes and a rapid decrease of
 192 the ICNC with height.

193 Figure 6 shows four time periods representing different conditions during the 4 Febru-
 194 ary. For the vertical profiles obtained between 1910 and 2010 UTC (Fig. 6 first row),
 195 when the SOB was not in cloud, the ICNCs have their maximum at a height of 2.5 m.
 196 The maximum ICNC at this height reaches up to 600 l⁻¹. For three of the profiles, the
 197 ICNC decrease by more than a factor of 5 from over 100 l⁻¹ at 2.5 m to less than 20 l⁻¹ at
 198 10 m. The mean ICNC decreases from around 100 l⁻¹ at 2.5 m to 10 l⁻¹ at 10 m (Fig. 6,
 199 right panel in the first row). The large extend of the shaded area at 2.5 m represents the
 200 high variability of the ICNC even when the data is averaged over 50 holograms. Because
 201 the SBO was not in cloud during this time period, these measurements strongly suggest an
 202 influence by surface based processes at a wind speed of less than 10 m s⁻¹ of up to several
 203 hundreds of ice crystals per liter at a height of 2.5 m.

204 Between 2030 and 2200 UTC (Fig. 6 second row), when the SBO was in cloud
 205 again, the vertical profiles of the ICNC show a similar tendency as in the cloud free pe-
 206 riod. The maximum of the ICNC was observed at a height of 4.1 m and the ICNC de-
 207 creases consistently for all four profiles with height above the observed maximum. The
 208 boxplot on the right of Figure 6 shows that the mean of the ICNC decreases by a factor
 209 of 9 from its maximum at 4.1 m to its minimum at 10 m. This decrease is in the same or-

der of magnitude as in the cloud free case discussed above. Assuming that the observed ICNC at 10 m is representative for the cloud without surface influence, the surface-based processes contribute with several hundreds of ice crystals per liter to the measurements at 2.5, 4.1 and 6.0 m. This surface-based contribution is in the same order of magnitude as the total measured ICNCs in the cloud free period observed between 1910 and 2020 UTC. The influence extends to a height of 6.0 m, which is probably due to an increased wind speed of up to 15 m s^{-1} .

The highest ICNCs were observed in the time period between 1200 and 1500 UTC (Fig. 6 second row) when also the wind speed reaches its maximum of 25 m s^{-1} . The box-plot for this time interval shows a maximum ICNC at 2.5 m in the range of 500 to 900 l^{-1} and a decrease by a factor of 2 within 7.5 m. This decrease is much lower than observed in the previous time interval and is most likely due to the high wind speeds. Between different profiles the ICNC changed by a factor of, however, the trend of a decreasing ICNC with height was observed consistently for all profiles.

In the morning between 8300 and 1100 UTC the observed ICNCs (Fig. 6 first row) are much lower than between 1200 and 1500 UTC, although wind speed was as high as 20 m s^{-1} . A possible reason is the history of the snowpack before 04 February 2017. The last snow fall was observed on ?? February 2017 and most of the loose ice crystals on top of the snowpack possibly already have been blown away. Therefore, higher wind speeds are necessary to resuspend ice crystals from the snowpack.

To get an estimate of the correlation between wind speed and ICNC, the ICNC is averaged over a time interval of 1 min and compared to the maximum wind speed in the corresponding 1 min time interval observed by the SBO on top of the meteorological tower. Maximum wind speed is used rather the average wind speed, because it is expected that the gusts, i.e. the highest wind speed in an time interval are most relevant for resuspending ice crystals from the surface. For the time interval between 0830 an 1500 UTC when the wind direction was west-southwest (Fig 7, top) the ICNC shows no strong correlation is observed for wind speeds higher than 14 m s^{-1} . For the time interval bwetween 1910 and 2230 UTC (Fig 7, bottom), when the wind direction was north, a much more pronounced dependency of the ICNC on wind speed is observed for wind speeds lower than 14 m s^{-1} . This is a possible indication that the ice crystal concentration reaches a saturation for wind speed larger than 14 m s^{-1} for the conditions on 04 February 2014.

3.2 17 February 2017

On 17 February a cold front over northern Europe was moving southwards causing mainly northerly flow across the alps and at the SBO. Wind speeds observed at the SBO in the time interval between 1800 and 2000 UTC were between 5 and 10 m s^{-1} (Fig. 4). In the same time interval temperature decreased by 1 K from -12.5 to -13.5°C . The SBO was in cloud starting from 1300 UTC with varying visibility between several meters up to several hundreds of meters. Some snow fall was observed in the afternoon between 1300 and 1500 UTC.

For this day wind data of the 3D Sonic Anemometer are available, which allow a more detailed analysis of the correlation between the observed ICNC and wind speed. Unfortunately, only four vertical profiles were obtained with the HoloGondel platform due to hardware problems with the computer of the platform. The first profile was measured in the morning at 1200 UTC when the SBO was not in cloud and no ice crystals were observed. Three more profiles were observed in the late afternoon starting from 1800 UTC. For these profiles the ice crystals have been classified by hand and subclassified in the three categories: regular, irregular and aggregates.

Figure 8 gives an overview on the three profiles observed in the late afternoon of 17 February. An ICNC of several hundreds was observed in the lowest height intervals

with a maximum between 4.1 and 6.0 m. The minimal ICNC was consistently observed for all profiles at 10 m and was always below 150 l^{-1} . The decrease of the ICNC varies between a factor of 2 and 4. In general the observed profiles on this day are similar to the ones observed on 4 February between 2030 and 2200 UTC. This may be explained by very similar meteorological conditions. Wind direction was mainly from North to Northeast and wind speed varied between 5 and 10 m s^{-1} in both measurement intervals. Only temperature was slightly lower on 17 February.

In Figure 9 ICNCs are compared to various wind speeds. In contrast to the data of 4 February no correlation between ICNCs and the horizontal wind speed is observed. This holds true for the one minute average and maximum wind speed of the corresponding time interval observed by the SBO as well as the secondly average observed with the 3D Sonic Anemometer from the HoloGondel Platform. However, Figure 9c shows an increase of ICNC with the vertical wind speed.

All the ice crystals observed on 17 February were classified by hand a subclassification into irregular and regular ice crystals as well as aggregates was realized. The profiles of the subcatogized ICNCs and the relative abundance of these categories on the different heights are shown in Figure 10. ICNCs are dominated by irregular ice crystals, which is in good agreement with various other observations (citations). However, it is surprising to us that the relative importance of the irregular ice crystals stays constant with height or even increases. From surface based ice crystal enhancement processes irregular are ice crystals are expected to enhance ICNCs near the surface. With increasing height this influence is expected to decrease and regular ice crystals to become more important. However, from this data a proportional decrease of the absolute number of regular and irregular ice crystals is observed. In Figure 11 the concentration of the different habits is correlated to the vertical wind speed observed. It shows that the ICNC of irregular ice crystals dependence more on wind speed.

Figure 12 shows the size distribution of regular and irregular ice crystals at three different heights. Whereas the shape of the size distribution of the irregular ice crystals doesn't vary much and only decreases with height, the size distribution of the regular ice crystals shows a stronger decrease of the larger ice crystals.

4 Discussion

4.1 Wind dependency of the observed ICNCs

The observations on 4 February and 17 February show a different correlation of the ICNC with wind speed. Whereas the ICNCs observed on 4 February show a dependency on horizontal wind speed below 14 m s^{-1} , this dependency is not observed for ICNCs on 17 February 9. However for the data on 17 February a correlation is observed with vertical wind speed available from the 3D Sonic Anemometer. Because the vertical wind speed is not available for 17 February possible reasons for this observation are speculative. Possibly the orography plays an important role for the wind speed dependency. The north side of the SBO is a steep wall of 800 m. Therefore, vertical winds may transport ice crystals from this wall up to the ridge of the mountain, where they finally become lifted into the air. A possible reason for the missing wind dependency on 4 February for horizontal wind speeds larger than 14 m s^{-1} is a saturation of the concentration of blowing snow.

In previous literature a wind dependency was observed for ICNCs smaller than $100 \mu\text{m}$, whereas larger ICNCs were wind independent [Lloyd *et al.*, 2015]. Blowing snow, receptively hoar frost were proposed as the underlying mechanisms for these observations. Based on our observations we propose that at mountain-top research station not only the horizontal wind speed may play an important role for the resuspension of ice crystals from

309 the surface, but also the vertical wind speed. This may be true particular for research stations
 310 like the Jungfraujoch, Switzerland and SBO, Austria with their steep orography.

311 It has to be mentioned that various difficulties exist when it comes to observe the
 312 correlation between wind speed and ICNC. Firstly, ICNCs are usually compared to a si-
 313 multaneously measured wind speed. However, the observed ice crystals may have been
 314 resuspended some time before the measurement and transported in the air for a short time.
 315 In this case the simultaneously observed wind speed is not necessarily the driving force of
 316 the process of particle lifting. Secondly, wind and ICNC measurements may be performed
 317 at two different locations. Especially at mountain-top research station with its many struc-
 318 tures, local turbulence responsible for the resuspension of the observed ice crystals may be
 319 not well represented by such a wind measurement. Thirdly, the ICNC does not only de-
 320 pend on wind speed, but also on age of the snow cover and atmospheric conditions and a
 321 possible correlation may suppressed in a data set with different snowpack and atmospheric
 322 conditions.

323 4.2 Size distribution

324 To better understand if the observed ice crystals are mainly resuspended particles
 325 from the surface the ice crystals observed on 17 February were subclassified into three
 326 different habits: regular, irregular and aggregates and the results are compared to previous
 327 studies about blowing snow. Because the main focus of blowing snow studies was the re-
 328 distribution of snow and its effect on road visibility, avalanche danger as well as mass and
 329 energy balance, they usually focused on limited height intervals (<2 m) above the snow
 330 surface. To our knowledge only *Nishimura and Nemoto* [2005] conducted measurements
 331 of the properties of blowing snow up to a height of 9.6 m at Mizuho Station, Antarctica.
 332 However, it is important to keep in mind that also this study was conducted over a flat sur-
 333 face in dry air conditions.

334 It is known that the particle size distribution at different heights can be well rep-
 335 resented with two-parameter gamma probability density functions [Budd, 2013; Schmidt,
 336 1982]

$$337 f(d) = \frac{d^{\alpha-1}}{\beta^\alpha \Gamma(\alpha)} \exp\left(-\frac{\beta}{d}\right) \quad (1)$$

338 with the particle diameter d , the shape parameter α and the scale parameter β . The
 339 fitted results for 17 February are shown in Figure 13 for both regular and irregular ice
 340 crystals. The fits show close agreement with the data for both habits and all heights. The
 341 resulting shape parameter α and the mean diameter, represented by the product of the
 342 shape and scale parameter of the gamma-pdf, are plotted in Figure 14. The mean diameter
 343 of the regular ice crystals decreases with increasing height from 120 to 70 μm , whereas
 344 the mean diameter of the irregular ice crystals is constant at 100 μm . The shape factor
 345 for the irregular ice crystals also varies only little, whereas the shape factor for the regu-
 346 lar ice crystals increases from 5 to 7 at a height of 10 m. Compared to the results of ??
 347 the parameters of the size distribution of the regular ice crystals compare much better to
 348 the properties of blowing snow than the of irregular crystals. This is puzzling, because
 349 blowing snow has been observed to have dominantly ice crystals of irregular habits (cita-
 350 tion). For the data observed between 1910 and 2000 UTC on 4 February, which is clearly
 351 a blowing snow event, inspection of the ice crystal habit by eye confirm these results.

352 II is not believed that the regular ice crystals observed on 17 February origin from
 353 the surface, because they show a much weaker wind dependency than irregular ice crys-
 354 tals (Fig. reffig:ICNCvsWindHabits1702). This is also observed during one vertical pro-
 355 file (Fig. 10, middle row). The vertical wind speed during this profile was similar for all
 356 heights (3 m s^{-1}), only when the elevator was at a height of 6 m a wind speed reached its

maximum of 4.5 m s^{-1} . Whereas the concentration of irregular ice crystals significantly increases at this time and height, the concentration of regular ice crystals gradually decreases with height. This suggests that ice crystals resuspended from the surface have irregular habits and are much more wind dependent.

In this case a different mechanism has to be responsible for the decrease if the ICNC of regular and irregular ice crystals observed on 17 February (Fig. 10). Possibly a turbulent layer above the surface enriches the ICNC of irregular as well as regular ice crystals. In this case surface-based ice-crystal enhancement processes only infrequently increase the ICNC irregular crystals as observed in one profile at a height of 6 m and on 4 February 2017. This also explains why a wind dependency was observed for the irregular ice crystals but not the regular ice crystals. If such an effect is responsible for the decrease of the ICNC, the differences in the size distribution of irregular and regular ice crystals can still not fully be explained. The differences between the irregular ice crystals and the observations of blowing snow by *Nishimura and Nemoto* [2005] is possibly due to the missing sublimation of ice crystals in cloud as it was observed in this study. This can explain the observation of a constant mean diameter with height, whereas the mean diameter in dry air decreased. An explanation of the decrease of the mean diameter of the regular ice crystals can not be given at this point and further observations are necessary to fully understand the findings of this study.

5 Conclusion

This study assess the potential influence of mountain-top in-situ measurements by surface-based ice-crystal enhancement processes and possible implications on the relevance of such measurements for atmospheric studies. For this, an elevator was attached to the meteorological tower of the SBO, Austria and vertical profiles of the ICNC were observed with the holographic imager HOLIMO on two days in February 2017. The main findings are:

- A decrease of the ICNC by at least a factor of two is observed, if the maximum ICNC is larger than 100 l^{-1} . This decrease extended up to one order of magnitude during in cloud conditions and reached its maximum of more than two orders of magnitudes when the station was not in cloud.
- Irregular ice crystals show a stronger wind dependency than regular ice crystals. This is agreement with the observation that surface-based ice-crystals enhancement processes dominantly produce irregular ice crystals.
- On 17 February a similar decrease of the concentration of irregular and regular ice crystals is observed, which can not be explained by surface-based ice crystal enhancement processes. Possibly turbulent layer close to the surface contributes to an enriched ICNC.
- Based on the results of this study, in-situ measurements of the ICNC at mountain-top research stations close to the surface over estimate the ICNC by at least a factor of two. This limits the atmospheric relevance of such measurements. However, the data set obtained is to small to make a clear statement under which conditions in-situ measurements at mountain-top research station may well represent the real properties of a cloud in contact with the surface and when not.
- Further and more extensive field campaigns are necessary to better understand the mechanisms, which are responsible for the enhanced ICNC observed close to the surface at mountain-top research stations. Especially the reason for an increased concentration of irregular ice crystals near the surface is not understood. We propose to perform measurements with a tethered balloon system to extend vertical profiles and better understand possible mechanisms, which enhance the ICNC observed at mountain-top research stations.

407 **Acronyms**

- 408 **ICNC** Ice Crystal Number Concentration
 409 **HOLIMO** HOLographic Imager for Microscopic Objects
 410 **SBO** Sonnblick Observatory

411 **Acknowledgments**

412 Sonnblick Observatory and team (Elke Ludewig, Hermann Scheer, Norbert Daxbacher,

413 Lug Rasser, Hias Daxbacher)

414 Thanks to Hannes, Olga, Fabiola, Monika, for their help

415 Thanks to Rob for many discussions

416 **References**

- Baumgardner, D., J. Brenguier, A. Bucholtz, H. Coe, P. DeMott, T. Garrett, J. Gayet, M. Hermann, A. Heymsfield, A. Korolev, M. KrÃdmer, A. Petzold, W. Strapp, P. Pilewskie, J. Taylor, C. Twohy, M. Wendisch, W. Bachalo, and P. Chuang (2011), Airborne instruments to measure atmospheric aerosol particles, clouds and radiation: A cook's tour of mature and emerging technology, *Atmos. Res.*, 102(1â€§2), 10 – 29, doi:10.1016/j.atmosres.2011.06.021.
- Beck, A., J. Henneberger, S. Schöpfer, J. Fugal, and U. Lohmann (2017), Hologondel, *Atmos. Meas. Tech.*
- Bromwich, D. H. (1988), Snowfall in high southern latitudes, *Reviews of Geophysics*, 26(1), 149–168, doi:10.1029/RG026i001p00149.
- Budd, W. F. (2013), *The Drifting of Nonuniform Snow Particles1*, pp. 59–70, American Geophysical Union, doi:10.1029/AR009p0059.
- Déry, S. J., and M. K. Yau (1999), A climatology of adverse winter-type weather events, *Journal of Geophysical Research: Atmospheres*, 104(D14), 16,657–16,672, doi: 10.1029/1999JD900158.
- Farrington, R. J., P. J. Connolly, G. Lloyd, K. N. Bower, M. J. Flynn, M. W. Gallagher, P. R. Field, C. Dearden, and T. W. Choularton (2015), Comparing model and measured ice crystal concentrations in orographic clouds during the inupiaq campaign, *Atmos. Chem. and Phys.*, 15(18), 25,647–25,694, doi:10.5194/acpd-15-25647-2015.
- Field, P. R., R. P. Lawson, P. R. A. Brown, G. Lloyd, C. Westbrook, D. Moisseev, A. Miltenberger, A. Nenes, A. Blyth, T. Choularton, P. Connolly, J. Buehl, J. Crosier, Z. Cui, C. Dearden, P. DeMott, A. Flossmann, A. Heymsfield, Y. Huang, H. Kalesse, Z. A. Kanji, A. Korolev, A. Kirchgaessner, S. Lasher-Trapp, T. Leisner, G. McFarquhar, V. Phillips, J. Stith, and S. Sullivan (2017), Secondary ice production: Current state of the science and recommendations for the future, *Meteorological Monographs*, 58, 7.1–7.20, doi:10.1175/AMSMONOGRAPH-D-16-0014.1.
- Fugal, J. P. (2017), Holosuite, in preparation.
- Geerts, B., B. Pokharel, and D. a. R. Kristovich (2015), Blowing Snow as a Natural Glaciogenic Cloud Seeding Mechanism, *Mon. Weather Rev.*, 143(12), 5017–5033, doi: 10.1175/MWR-D-15-0241.1.
- Gultepe, I., G. Isaac, and S. Cober (2001), Ice crystal number concentration versus temperature for climate studies, *International Journal of Climatology*, 21(10), 1281–1302, doi:10.1002/joc.642.
- Hallet, J., and S. Mossop (1974), Production of secondary ice particles during the riming process, *Nature*, 249, 26–28, doi:10.1038/249026a0.
- Lachlan-Cope, T., R. Ladkin, J. Turner, and P. Davison (2001), Observations of cloud and precipitation particles on the avery plateau, antarctic peninsula, *Antarctic Science*, 13(3), 339â€§348, doi:10.1017/S0954102001000475.

- 455 Li, L., and J. W. Pomeroy (1997), Estimates of threshold wind speeds for snow trans-
 456 port using meteorological data, *Journal of Applied Meteorology*, 36(3), 205–213, doi:
 457 10.1175/1520-0450(1997)036<0205:EOTWSF>2.0.CO;2.
- 458 Lloyd, G., T. W. Choularton, K. N. Bower, M. W. Gallagher, P. J. Connolly, M. Flynn,
 459 R. Farrington, J. Crosier, O. Schlenczek, J. Fugal, and J. Henneberger (2015), The ori-
 460 gins of ice crystals measured in mixed-phase clouds at the high-alpine site jungfraujoch,
 461 *Atmos. Chem. Phys.*, 15(22), 12,953–12,969, doi:10.5194/acp-15-12953-2015.
- 462 Lohmann, U. (2002), Possible aerosol effects on ice clouds via contact nucle-
 463 ation, *Journal of the Atmospheric Sciences*, 59(3), 647–656, doi:10.1175/1520-
 464 0469(2001)059<0647:PAEOIC>2.0.CO;2.
- 465 Mahesh, A., R. Eager, J. R. Campbell, and J. D. Spinhirne (2003), Observations of blow-
 466 ing snow at the south pole, *Journal of Geophysical Research: Atmospheres*, 108(D22),
 467 n/a–n/a, doi:10.1029/2002JD003327, 4707.
- 468 Nishimura, K., and M. Nemoto (2005), Blowing snow at mizuho station, antarctica, *Phi-
 469 losophical Transactions of the Royal Society of London A: Mathematical, Physical and En-
 470 gineering Sciences*, 363(1832), 1647–1662, doi:10.1098/rsta.2005.1599.
- 471 Palm, S. P., Y. Yang, J. D. Spinhirne, and A. Marshak (2011), Satellite remote sensing of
 472 blowing snow properties over antarctica, *Journal of Geophysical Research: Atmospheres*,
 473 116(D16), n/a–n/a, doi:10.1029/2011JD015828, d16123.
- 474 Rangno, A. L., and P. V. Hobbs (2001), Ice particles in stratiform clouds in the arctic and
 475 possible mechanisms for the production of high ice concentrations, *Journal of Geophysi-
 476 cal Research: Atmospheres*, 106(D14), 15,065–15,075, doi:10.1029/2000JD900286.
- 477 Rogers, D. C., and G. Vali (1987), Ice crystal production by mountain sur-
 478 faces, *J. Clim. Appl. Meteorol.*, 26(9), 1152–1168, doi:10.1175/1520-
 479 0450(1987)026<1152:ICPBMS>2.0.CO;2.
- 480 Rotunno, R., and R. A. Houze (2007), Lessons on orographic precipitation from the
 481 mesoscale alpine programme, *Quarterly Journal of the Royal Meteorological Society*,
 482 133(625), 811–830, doi:10.1002/qj.67.
- 483 Schlenzeck, O., and J. Fugal (2017), Microphysical properties of ice crystal precipitation
 484 and surface-generated ice crystals in a high alpine environment in switzerland, *esult*, 56,
 485 433–453, doi:10.1175/JAMC-D-16-0060.1.
- 486 Schmidt, R. A. (1982), Vertical profiles of wind speed, snow concentration, and
 487 humidity in blowing snow, *Boundary-Layer Meteorology*, 23(2), 223–246, doi:
 488 10.1007/BF00123299.
- 489 Vali, G., D. Leon, and J. R. Snider (2012), Ground-layer snow clouds, *Quarterly Journal
 490 of the Royal Meteorological Society*, 138(667), 1507–1525, doi:10.1002/qj.1882.
- 491 Vionnet, V., G. GuyomarcâŽh, F. N. Bouvet, E. Martin, Y. Durand, H. Bellot, C. Bel,
 492 and P. PugliaÃlise (2013), Occurrence of blowing snow events at an alpine site over a
 493 10-year period: Observations and modelling, *Advances in Water Resources*, 55, 53 – 63,
 494 doi:<http://doi.org/10.1016/j.advwatres.2012.05.004>, snowâŠAtmosphere Interactions
 495 and Hydrological Consequences.
- 496 Yang, J., and M. K. Yau (2008), A new triple-moment blowing snow model, *Boundary-
 497 Layer Meteorology*, 126(1), 137–155, doi:10.1007/s10546-007-9215-49.

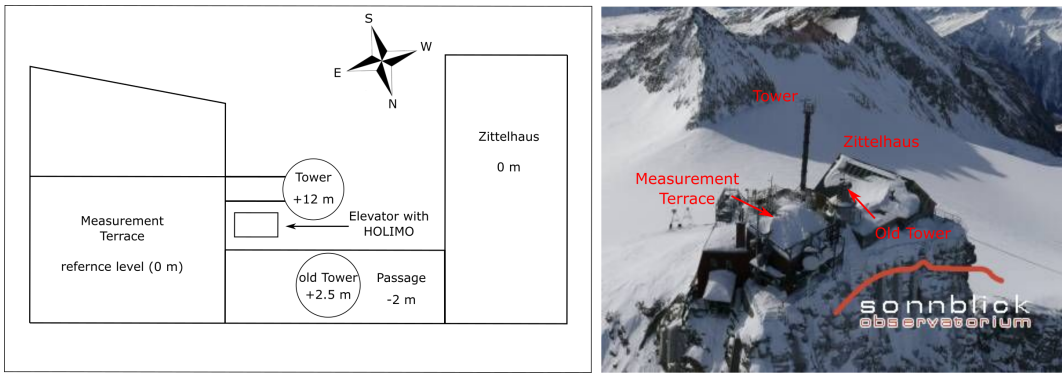


Figure 1. Sketch of the experimental setup and the surrounding structures (left) with their heights relative to the bottom of the measurement terrace. Aerial image of the Sonnblick Observatory (right).

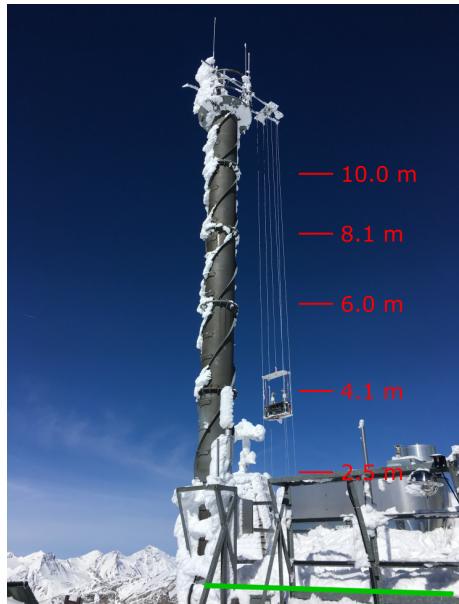
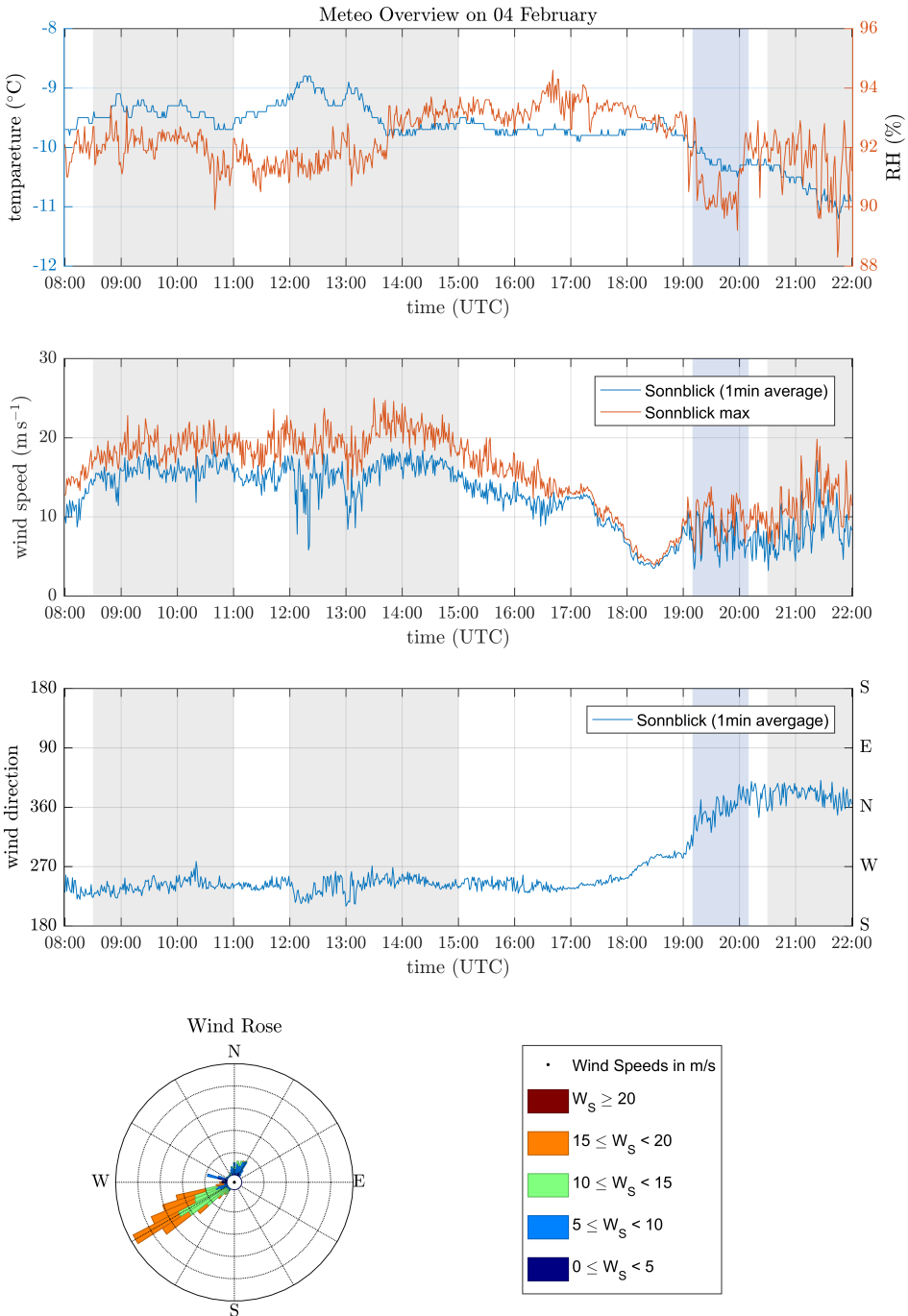
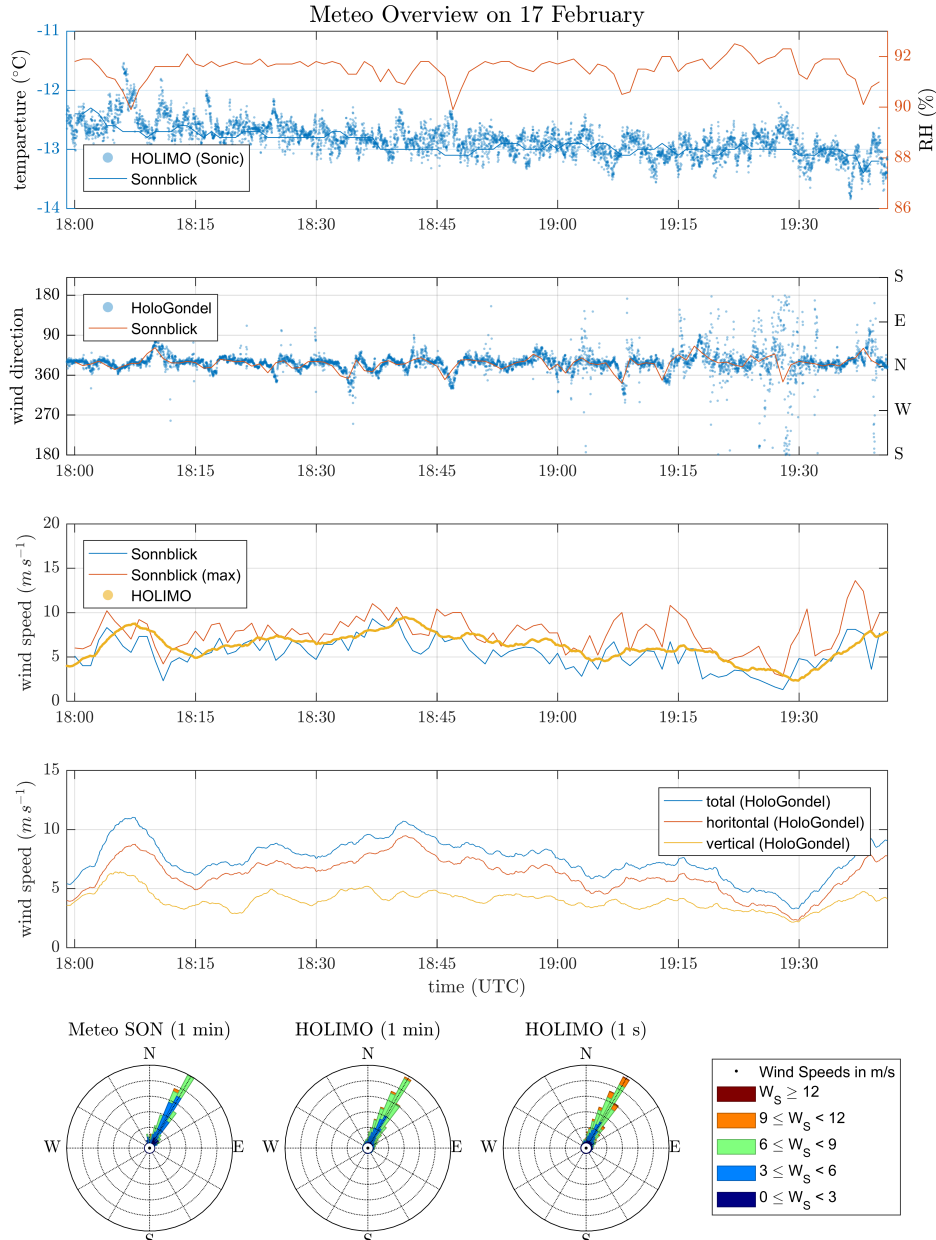


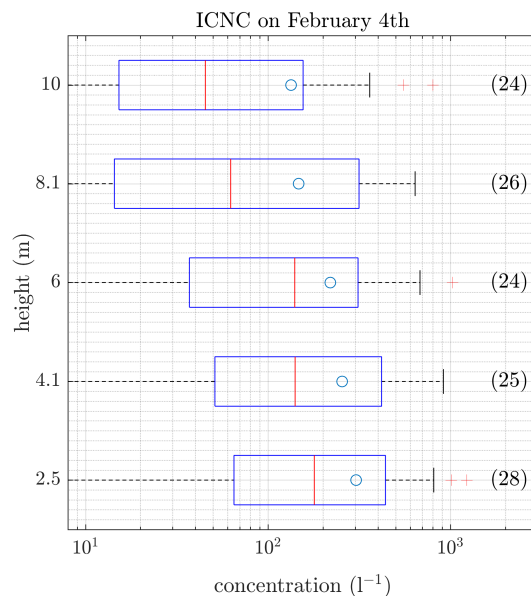
Figure 2. Set up of the elevator with the holographic imager HOLIMO mounted to the meteorological tower at the SBO. The red lines and numbers indicate the five different heights where the elevator was positioned repeatedly to obtain vertical profiles of the ICNC. The reference height of 0.0 m is the bottom of the measurement platform (green line).



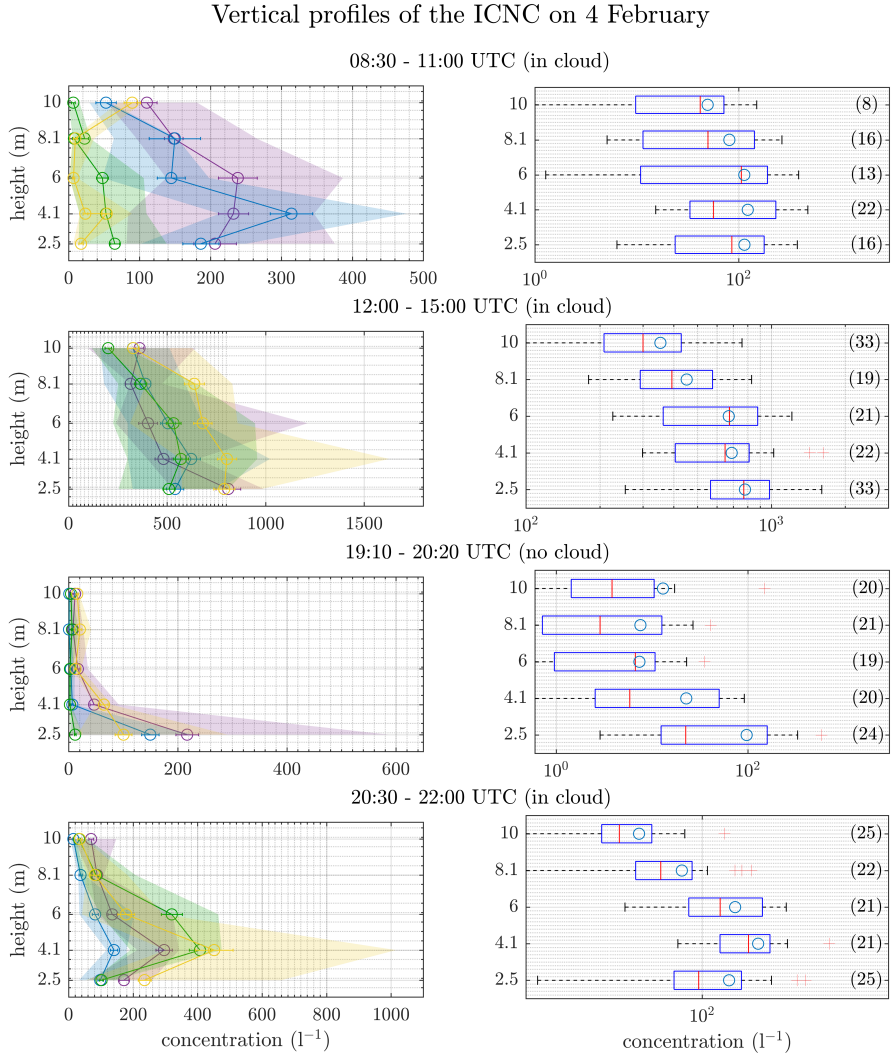
504 **Figure 3.** Overview of the meteorological conditions on 4 February obtained from the SBO measurements.
 505 Shown are the temperature, relative humidity (top), wind speed (second from top) and wind direction (second
 506 from bottom). All measurements are 1 min averages except for the maximum wind speed, which corresponds
 507 to the maximum wind speed observed during a corresponding 1 min average. Grey and blue shaded areas
 508 represent time with measurement (see Fig. 6) when the SBO was in cloud, respectively not in cloud. A wind
 509 rose plot (bottom) of the wind measurement is also shown.



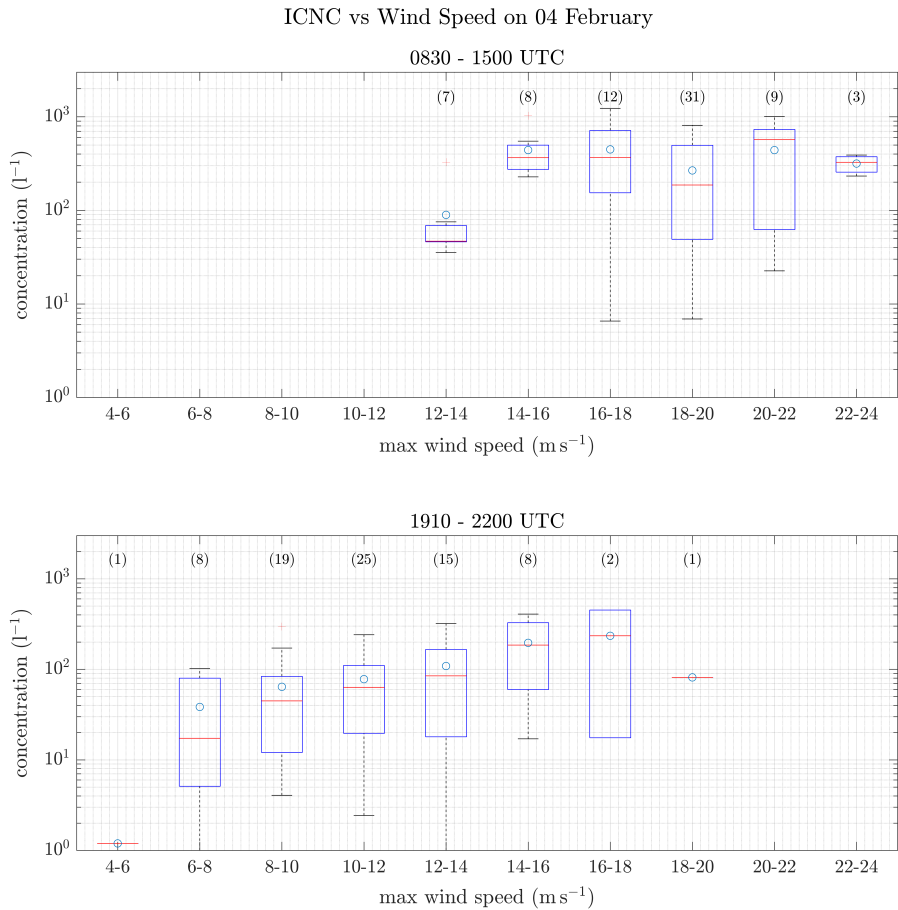
510
 511 **Figure 4.** Overview on the meteorological conditions on 17 February for the time interval when measure-
 512 ments exist (see Fig. 8). On this day temperature and wind measurements are available from the SBO and the
 513 3D Sonic Anemometer. Shown are the temperature and relative humidity (top), wind direction (second from
 514 top), a comparison of the horizontal wind speed (middle) and detailed wind speed measurements from the 3D
 Sonic Anemometer (second from bottom). A windrose plot is shown in the bottom panel.



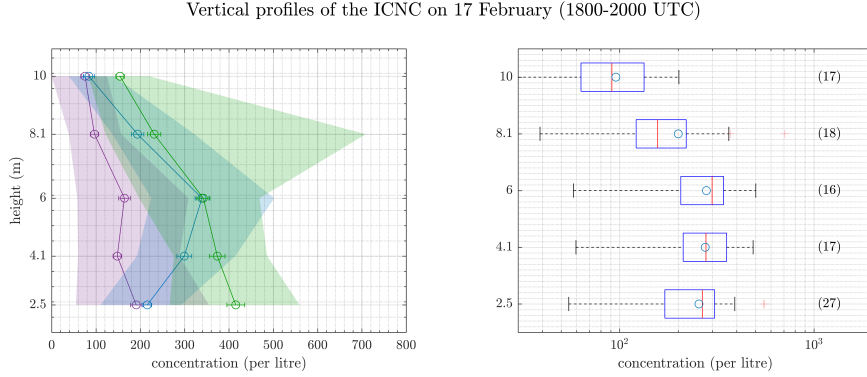
515 **Figure 5.** ICNC as a function of the height of the elevator at the meteorological tower of the SBO. This plot
 516 is a summary of the 24 profiles obtained on 4 February. The data was averaged over the entire time period
 517 of single measurements at the different height. The number in brackets is the number of concentration
 518 measurements per height. For each box, the central line marks the median value of the measurement and the
 519 left and right edges of the box represent 25th and the 75th percentiles respectively. The whiskers extend to
 520 minimum and maximum of the data; outliers are marked as red pluses. The mean value of the measurements
 521 is indicated as a blue circle.



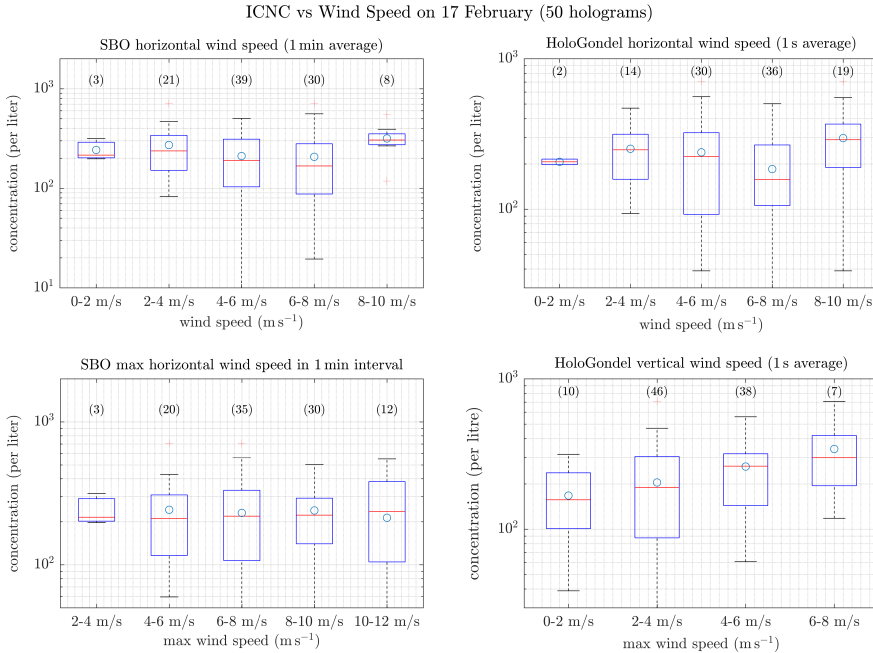
522 **Figure 6.** ICNCs as a function of height of the elevator for four different time intervals during 4 February,
 523 representing different conditions (Fig. 3). On the individual profiles (left), the circles indicate the mean value
 524 averaged over the entire time interval. The error bars represent the standard error of the mean. The shaded
 525 area extends from the minimum to the maximum of the measured ICNC. As in Fig. 5 only for the four time
 526 intervals the box plots (right) show a summary of the data.



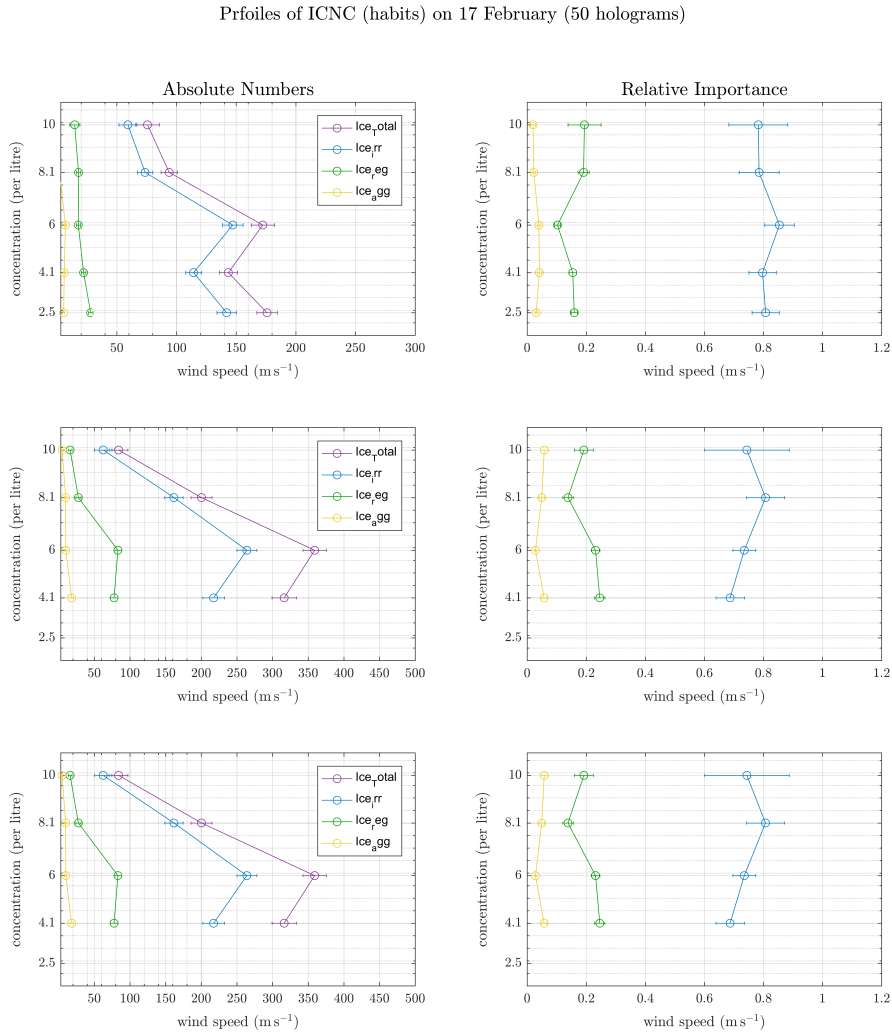
527 **Figure 7.** As Figure 5 only ICNC as a function of horizontal wind speed for the the time periods between
 528 0830 and 1500 UTC when the wind direction was West-Southwest (top) and between 1910 and 2200 UTC
 529 when the wind direction was North (bottom). The wind speed is the maximum wind speed in one minute time
 530 intervals from the SBO.



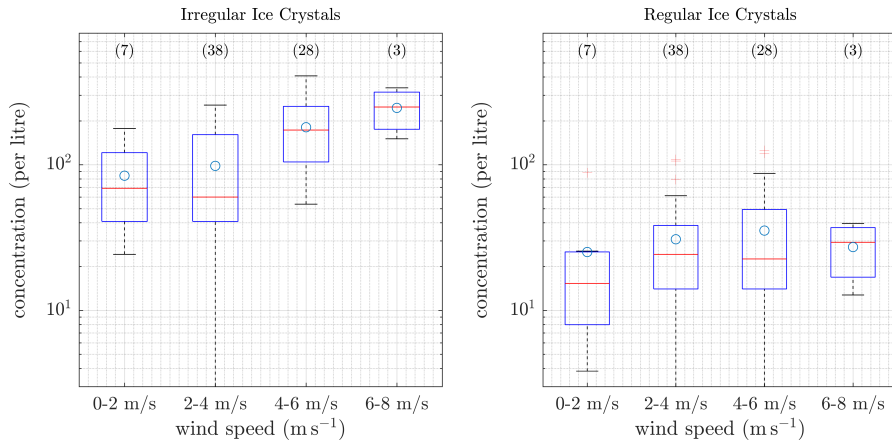
531 **Figure 8.** Ice crystal number concentration as a function of the height of the elevator at the meteorological
 532 tower of the SBO for 17 February. On the left are the three individual profiles obtained in cloud. The circles
 533 indicate the mean value averaged over the entire time interval. The error bars represent the standard error of
 534 the mean. The shaded area indicates the variability of the data and extends from the minimum to the maxi-
 535 mum when the data is averaged over 50 holograms. For the summary of the different time intervals (right) the
 536 data is averaged over 50 holograms. For each box, the central line marks the median value of the measurement
 537 and the left and right edges of the box represent 25th and the 75th percentiles respectively. The whiskers
 538 extend to minimum and maximum of the data; outliers are marked as red pluses.



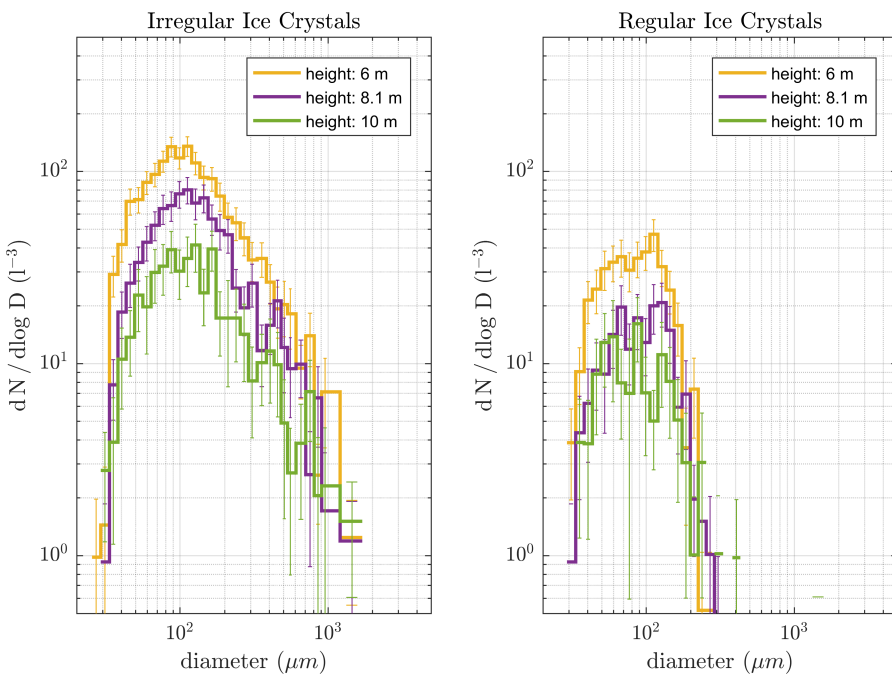
539 **Figure 9.** As Figure 7 only for 17 February and four different wind speed measurements: a) one minute
 540 averages of the horizontal wind speed from the SBO, b) maximum wind speed of the a corresponding time
 541 interval in a), c) secondly averages of the horizontal wind speed and d) secondly average of the vertical wind
 542 speed both from the 3D Sonic Anemometer.



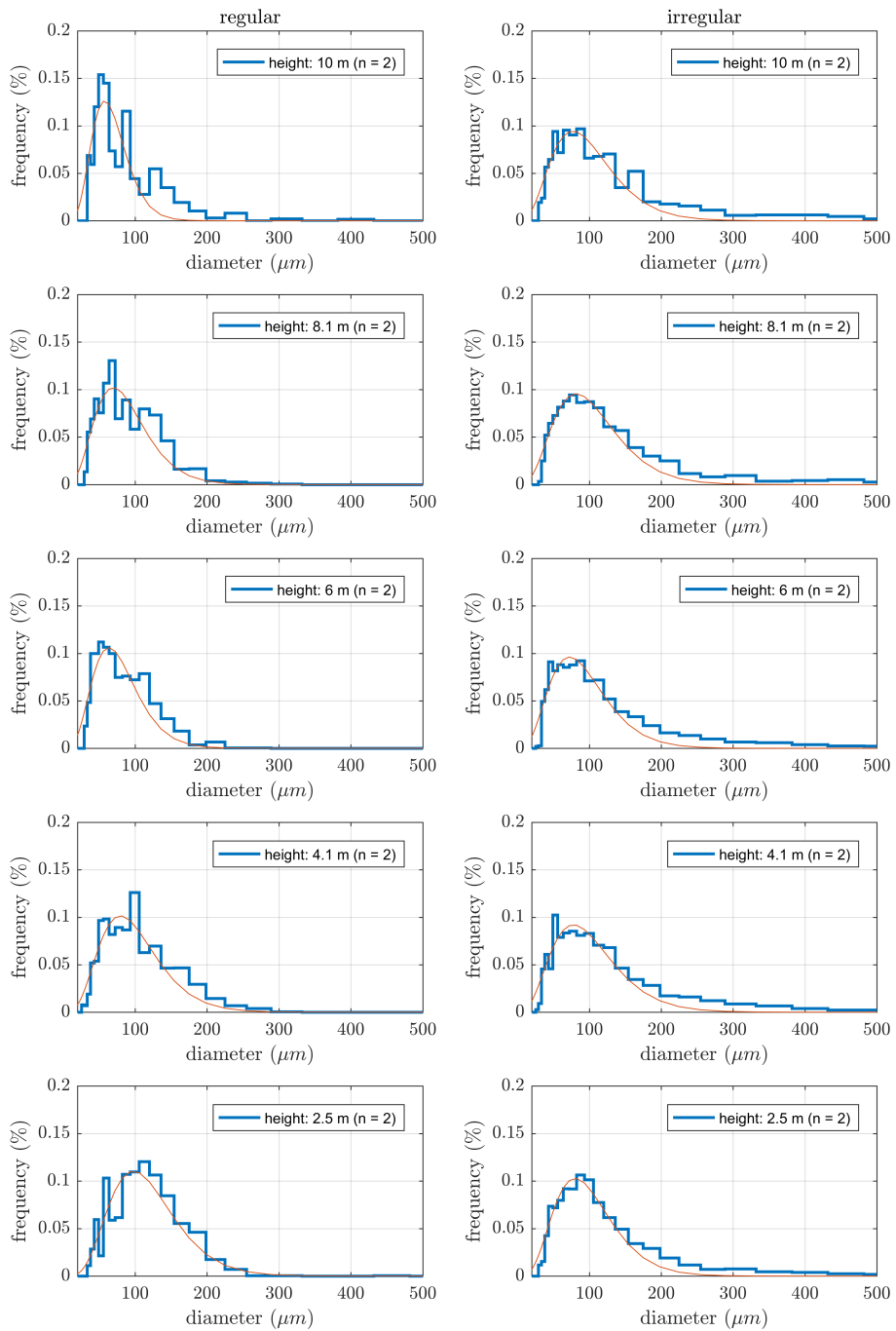
543 **Figure 10.** Vertical profiles of the concentration (left) and the relative importance (right) of the subclassified
 544 ice crystal habits: regular, irregular and aggregates. For the relative importance the number of ice crystals
 545 of different habits were divided by the total number of ice crystals. For theses plots the data as averaged
 546 over 50 holograms. In both cases the circles represent the mean of the 50 hologram averages. The error bars
 547 represent the standard error of the mean.



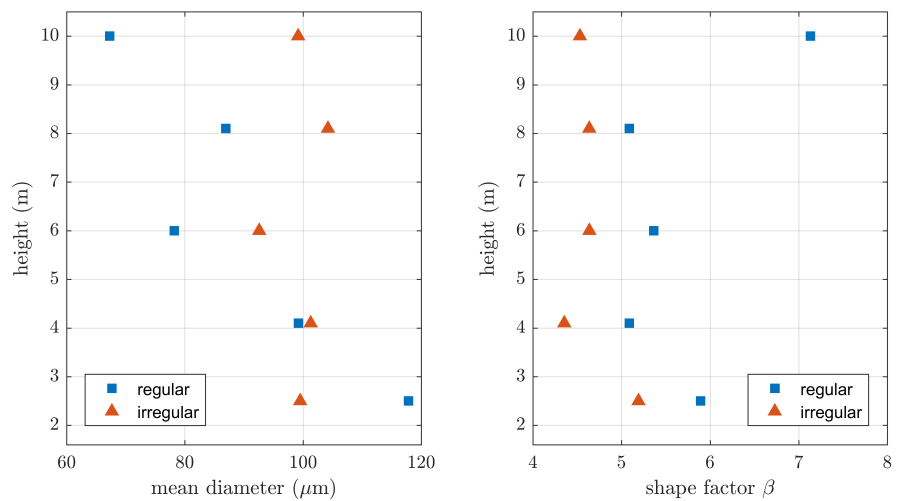
548 **Figure 11.** As Figure 7 only for 17 February and the ICNC of different ice crystal habits as a function of the
549 vertical wind speed.



550 **Figure 12.** Size distribution of the irregular (left) and regular (right) ice crystals observed on 17 February
551 as a function of height. The errorbars represent the standard error of the mean.



552 **Figure 13.** Probability distribution of the particle diameter for regular (left)
 553 and irregular (right) ice crystals
 554 measured on 17 February. The red line indicates the result of the fit of the two parameter gamma-pdf from
 equation (1).



555 **Figure 14.** Profiles of the mean diameter (left) and the shape parameter (right) of the two parameter
 556 gamma-pdf (Eq. (1)) plotted as a function of height.